

Investigation of Reinforced Acrylonitrile Butadiene Styrene Collimator on Single Photon Emission Computed Tomography Scanner Image Quality Parameters

¹Falade, O.A., ²Oni, O.M., ³Oni, E.A. & ⁴Aremu, A.

Department of Pure and Physics
Ladoke Akintola University of Technology
Ogobomoso, Oyo State, Nigeria

E-mails: faladeo56@gmail.com, omoni@lautech.edu.ng, eaoni53@lautech.edu.ng, aaremu37@lautech.edu.ng

ABSTRACT

This study examines the potential of reinforced Acrylonitrile Butadiene Styrene (ABS) composites as alternatives to lead collimators in Single Photon Emission Computed Tomography (SPECT), addressing issues such as lead's toxicity, cost, and manufacturing challenges in Low- and Middle-Income Countries (LMICs). Using Monte Carlo simulations with the Geant4 Applications for Tomographic Emission (GATE) toolkit, the performance of various materials, including reinforced ABS, Poly Lactic Acid (PLA), and tungsten, was evaluated using a Technetium-99m source at 140 keV with an activity of 1 and 400 MegaBecquerel. Lead collimators served as the baseline for comparison, with materials assessed for sensitivity, spatial resolution, and energy resolution. The results suggest that ABS reinforced with bismuth (ABS-Bi) and PLA offer high sensitivity and energy resolution, making them promising, cost-effective options for LMICs. While tungsten provides the best spatial resolution, its high cost and lower sensitivity limit its use in these regions. PLA-Bulk-Bi and iron steel, which offer a good balance of sensitivity and energy resolution at more affordable costs, are also viable alternatives. Overall, the study concludes that while alternative materials may not fully replace lead in high-end SPECT applications, ABS-Bi and PLA composites present valuable, cost-effective options for improving SPECT imaging in resource-constrained settings.

Keywords: SPECT, Monte, Carlo simulation code, GATE, Acrylonitrile Butadiene Styrene, Sensitivity, Spatial resolution, Energy resolution.

Aims Research Journal Reference Format:

Falade, O.A., Oni, O.M., Oni, E.A. & Aremu, A. (2024): Investigating Reinforced Acrylonitrile Butadiene Styrene Collimator on Spect Scanner Sensitivity. *Advances in Multidisciplinary and Scientific Research Journal* Vol. 10. No. 4. Pp 19-30. www.isteams.net/aimsjournal. dx.doi.org/10.22624/AIMS/V10N4P3

1. INTRODUCTION

Single Photon Emission Computed Tomography (SPECT) is a key imaging technique in nuclear medicine used for diagnosing and monitoring a range of medical conditions, including cardiovascular diseases, cancers, and neurological disorders[1]. Central to SPECT imaging is the gamma camera system, which includes essential components such as collimators, scintillation crystals, photomultiplier tubes (PMTs), and pulse height analyzers.

Collimators direct gamma photons emitted by the patient toward the detector, while scintillation crystals like sodium iodide (NaI) convert these photons into visible light. PMTs amplify the light into electrical signals, which are analyzed by the pulse height analyzer to determine photon energy and position [5][12][15]. Parallel-hole collimators are commonly used in clinical SPECT scanning for whole-body imaging, while fan-beam collimators are preferred for brain imaging. Key factors influencing collimator performance include hole diameter, hole length, distance from the source, and material properties. Lead, with its high atomic number (82) and density (11.34 g/cm³), is effective at absorbing high-energy radiation but poses significant health and environmental risks, prompting interest in alternatives [16]. Tungsten, with a higher density (19.25 g/cm³) and superior mechanical strength, offers excellent shielding but is more brittle and expensive [4]. Iron steel (7.85 g/cm³) and stainless steel, due to their strength and corrosion resistance, are cost-effective for structural components and direct shielding, though stainless steel's higher cost limits its use [2][13][17].

Poly(lactic acid) (PLA), a biodegradable thermoplastic, is being investigated for 3D printed radiation shielding, especially when combined with bismuth nanoparticles. While PLA offers environmental benefits and customizable designs, its lower density and tensile strength make it less effective for shielding high-energy radiation compared to metals. Although PLA composites show promise, they require further optimization to match the shielding performance of traditional materials like lead and tungsten. These developments highlight the potential for new, more sustainable shielding materials, though their scalability and durability still need extensive research [8][11].

Spatial Resolution (S.R) refers to the ability of a collimator to distinguish between two points and is typically expressed in millimeters (mm). It can be calculated using the formula.

$S.R (mm) = FWHM = 2.355 \times \sigma$. Where σ (sigma) is the standard deviation or the width of the Gaussian fit [6]. Sensitivity (S) measures the efficiency with which a collimator detects gamma rays, often quantified in counts per second per megabecquerel (cps/MBq).

$$\text{The sensitivity is calculated by the } S = \frac{C_{net}}{\text{Activity}} \quad [14]$$

.Energy Resolution, on the other hand, reflects the collimator's ability to differentiate between photons of different energies. It is expressed as a percentage and is given by the mean energy of the gamma rays detected. Higher energy resolution improves image quality by reducing background noise and allowing more accurate identification of specific energy peaks.

$$E.R = \frac{2.35 \times \sigma}{\text{Energy mean}} \quad [2]$$

2. METHODOLOGY

Monte Carlo-Based design and simulation

In this study, Monte Carlo simulations were conducted using the Geant4 Application for Tomographic Emission (GATE), an open-source extension of the Geant4 toolkit [10]. The virtual version of GATE (vGate 9.2) was used, running within the VirtualBox environment, which supports x86 and AMD64/Intel64 architectures. The vGate system includes compiled source code and data analysis tools like ROOT files, providing an interface for simulating medical imaging systems.

The GATE toolkit also features pre-built modules, such as the SPECT Head, which were used to design the geometry for the Symbian T2 SPECT/CT scanner [7]. The simulations were carried out with and without collimators, exploring different materials for the collimators. The study specifically modeled a low-energy all-purpose (LEAP) collimator, with geometry and dimensions based on existing literature for the same clinical SPECT scanner model [7]. Specifications for modeling the SPECT scanner were detailed in Table 3.1. These simulations aimed to assess the impact of collimator materials on the performance of the SPECT system.

Table 1: Specifications of the Symbian T2 SPECT/CT scanner

VOLUMES	MEASUREMENT
Detector Field of View (cm)	53.3x 38.7
Crystal size (mm)	591 x 445
Crystal thickness (mm)	9.5
Collimator type	LEAP(Low Energy All Purpose)
Hole Shape	Hexagonal
Hole Length (mm)	24.05
Septal thickness (mm)	0.22
Hole diameter (mm)	1.45

Design of the Volumes

The SPECT scanner design began with defining a "world" volume consisting of air, with dimensions of 100 cm along the x, y, and z axes, which encompassed all components. Inside this world, the SPECT head was positioned as a box filled with air, with dimensions of 5.76 cm (X), 46.34 cm (Y), and 61.44 cm (Z). The design also included a Low-Energy All-Purpose (LEAP) collimator created within the SPECT head, featuring hexagonal prism holes to allow gamma photon passage. The NaI (sodium iodide) crystal, defined within the SPECT head, measured 9.5 mm by 445 mm by 591 mm and was filled with NaI material. Additionally, a back-compartment volume was created for the photomultiplier tube (PMT) region, positioned behind the crystal. The simulation used an EM standard option 4 physics list and specific cut values for gamma photons, electrons, and positrons.

The SPECT scanner simulation was performed using a cylindrical Technetium 99m source emitting photons isotropically, placed at the center of cylindrical air and water phantoms. Data was acquired in planar mode for two activity levels (1 MBq and 400 MBq) over a fixed time slice of 5 seconds. The study examined various collimator materials, including lead, tungsten, stainless steel, iron steel, PLA, PLA-Bulk-Bi, PLA-Nano-Bi, and reinforced Acrylonitrile Butadiene Styrene (ABS) infused with bismuth. These materials were selected based on their potential use in 3D printing applications, and their properties were defined in the GATE materials database for the simulation. Table 3.2 outlines the detailed descriptions of these materials.

Systems Requirements

In this study, simulations and data acquisition were conducted by connecting a local machine to a remote virtual machine (vGate server) built using Oracle's VirtualBox software, running an Ubuntu 64-bit operating system. The local machine, a Windows 10 PC with an Intel Core i5 processor and 8 GB of RAM, accessed the vGate server through an internet connection. A shared folder was established via the VirtualBox Extension Pack for file transfer.

The vGate environment ran GATE version 9.2, along with supporting software such as ROOT 6.26.08, libtorch cxx11 1.7.0, and ITK v5.3.0 with module_RTK=ON, as well as additional tools like VTK v9.0.3, vV 1.4, and ImageJ (Fiji) for simulation and data analysis. This setup allowed efficient use of the GATE resources and seamless operation for the study.

Data Acquisition

This involved defining the crystal volume as a sensitive detector and utilizing the Digitiser to record photon hits within this volume, as per the GATE Monte Carlo manual (OpenGate Collaboration, 2023). Data were collected in ROOT format and analyzed using Python and C scripts from GATE version 9.2. The results included a graphical representation of the source's planar image, photon distribution, energy spectrum, and resolution curve, which provided insight into the performance of the gamma camera system. For data analysis, the collected hits were grouped based on the LEAP collimator parameters and classified according to the interacting processes encountered by the photons in the crystal. The energy spectrum and resolution curve were fitted to compute key metrics such as counts, mean, and sigma. These values were then used to evaluate the gamma camera's performance, focusing on sensitivity, spatial resolution (FWHM), and energy resolution for each collimator material.

3. RESULTS AND DISCUSSION

Validation of Simulated SPECT Scanner

Results of the simulation with the source (technetium 99m) in air and water phantom at an energy of 140KeV with an activity of 1 MBq and 400 MBq was used with the manufacturer's specified value in chapter three. Collimator materials (Lead, Tungsten, Iron Steel, Stainless Steel and Reinforced Acrylonitrile Butadiene Styrene (varying percentage of bismuth) were simulated with GATE Monte Carlo Toolkit. Using ana_SPECT_ROOT within GATE, the information about the Energy Spectrum, Detector counts, Resolution Curve, Sensitivity, Spatial Resolution and Energy Resolution were recorded.

Results

The energy spectrum, detector counts, and resolution curves was utilized to obtain values, which were then used to plot graphs (Figures 4.1 to 4.12) illustrating the sensitivity, spatial resolution, and energy resolution of various collimator materials. The choice of collimator material in a SPECT scanner affects sensitivity, spatial resolution, and energy resolution. Materials like PLA and ABS-Bi-2 enhance sensitivity, improving photon detection for clearer images. PLA-Nano-Bi provides good spatial resolution for sharp images, while ABS-Bi has broader resolution, leading to blurrier results.

PLA-Bulk-Bi and steel improve energy resolution, enhancing image contrast. ABS-Bi-1 offers high sensitivity, while tungsten excels in spatial resolution. PLA-Nano-Bi and ABS-Bi-6 perform well in both spatial and energy resolution. Steel, PLA, and ABS-Bi-1 provide the highest sensitivity, while tungsten offers the best spatial resolution. Using collimators like PLA-Bulk-Bi, ABS-Bi-5, and tungsten improves spatial resolution and image quality. High energy resolution from materials like tungsten, PLA, and ABS helps differentiate radionuclides.

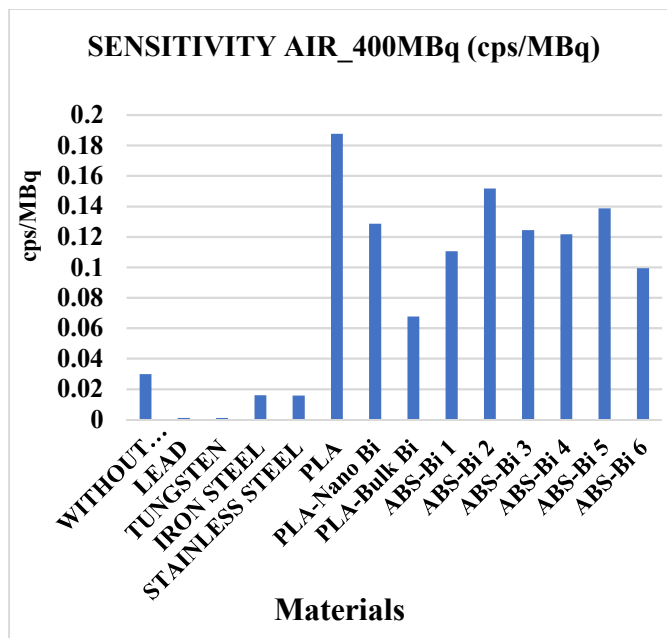


Figure 1: Sensitivity for all Collimator materials at an activity of 400 MBq and energy of 140 KeV of the source Tc-99m.

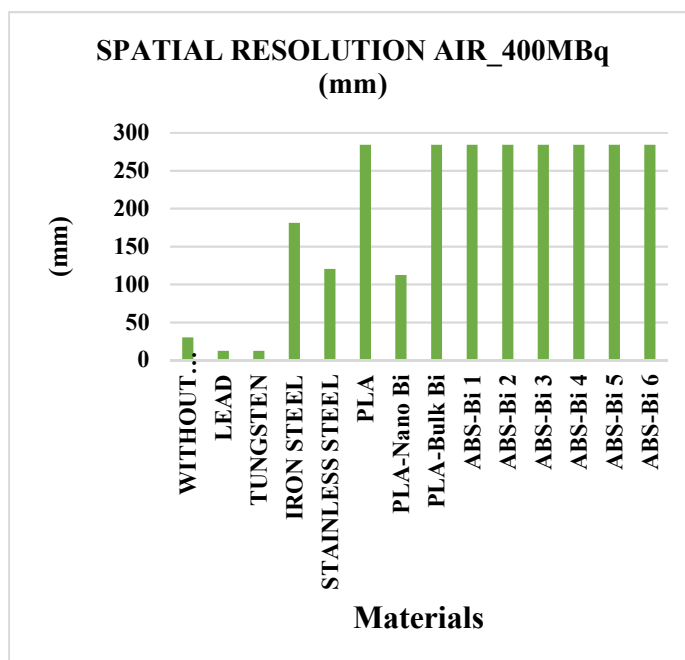


Figure 2: Spatial Resolution for all Collimator materials at an activity of 400 MBq and energy of 140 KeV of the source Tc-99m.

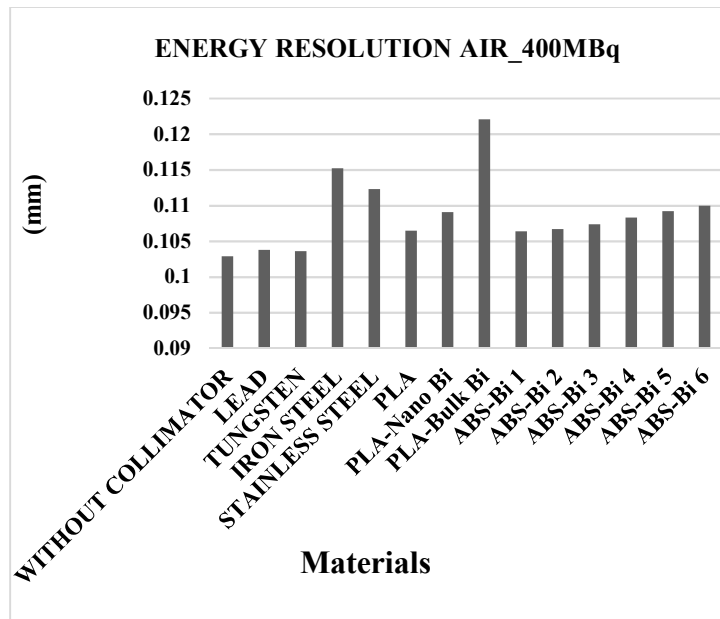


Figure 3: Energy Resolution for all Collimator materials at an activity of 400 MBq and energy of 140 KeV of the source Tc-99m.

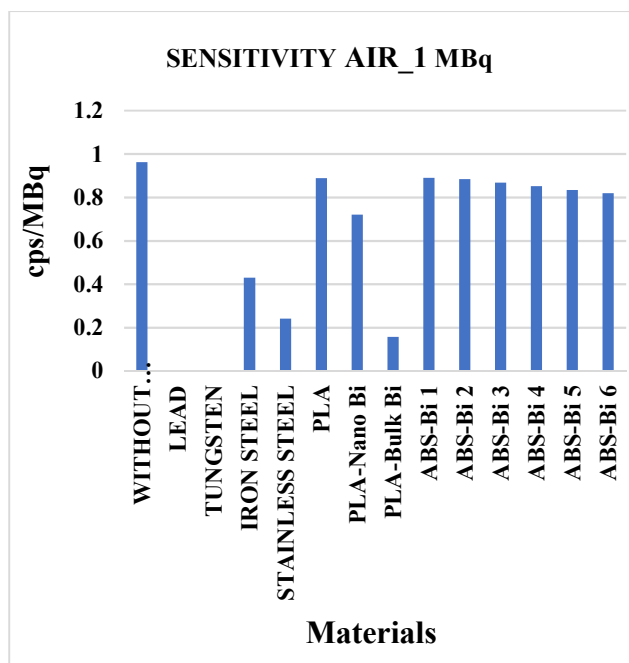


Figure 4: Sensitivity for all Collimator materials at an activity of 1 MBq and energy of 140 KeV of the source Tc-99m.

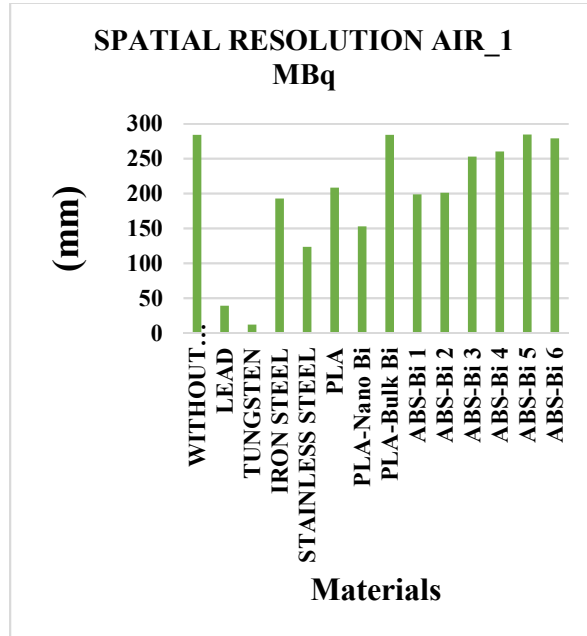


Figure 5: Spatial Resolution for all Collimator materials at an activity of 1 MBq and energy of 140 KeV of the source Tc-99m.

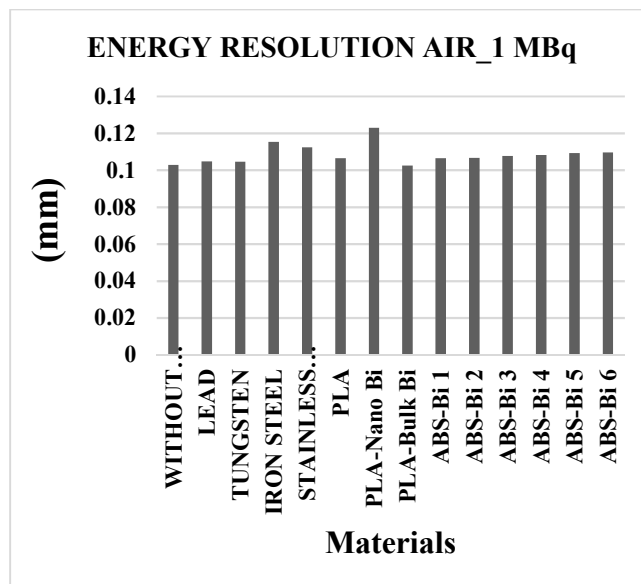


Figure 6: Energy Resolution for all Collimator materials at an activity of 1 MBq and energy of 140 KeV of the source Tc-99m.

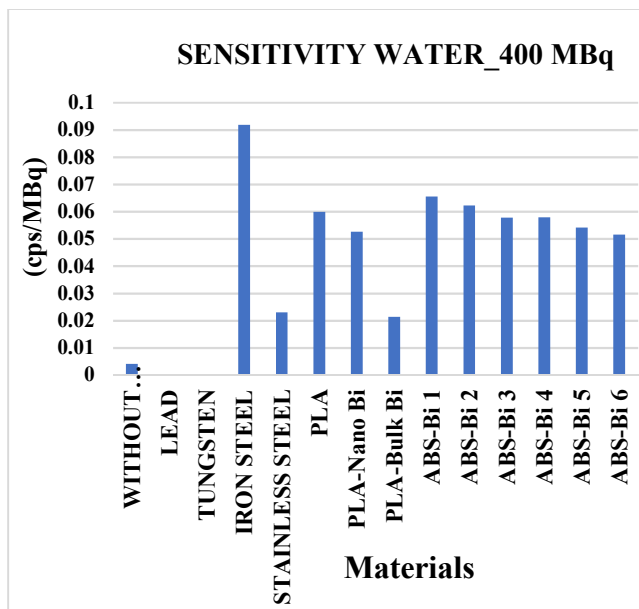


Figure 7: Sensitivity for all Collimator materials at an activity of 400 MBq and energy of 140 KeV of the source Tc-99m.

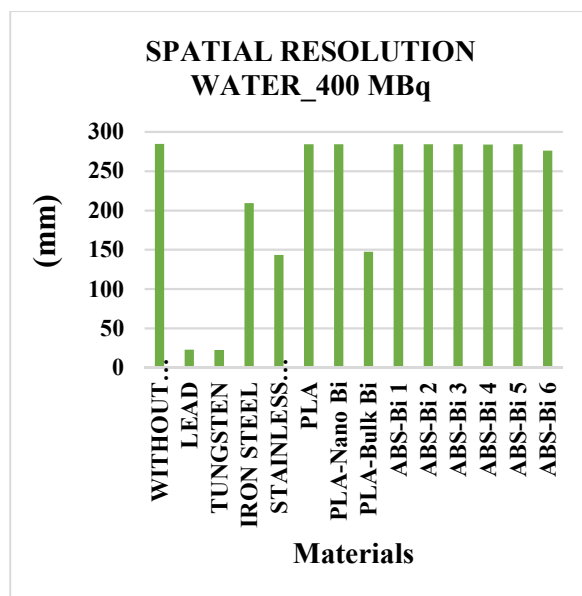


Figure 8: Spatial Resolution for all Collimator materials at an activity of 400 MBq and energy of 140 KeV of the source Tc-99m.

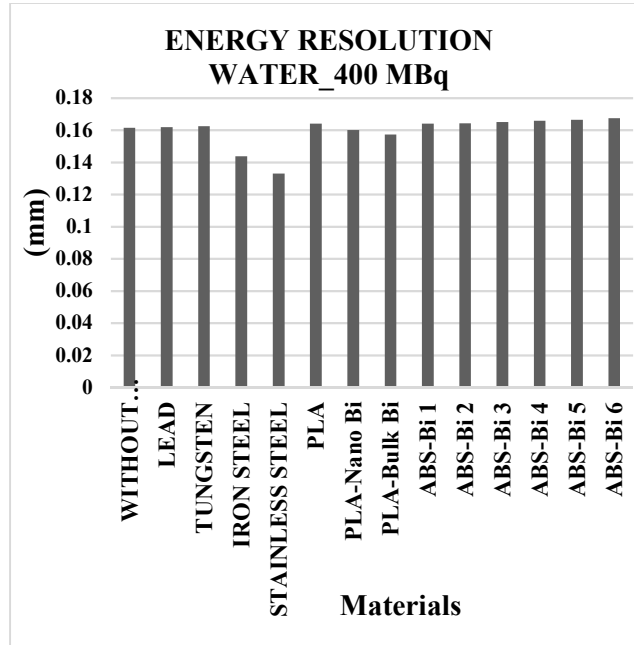


Figure 9: Energy Resolution for all Collimator materials at an activity of 400 MBq and energy of 140 KeV of the source Tc-99m.

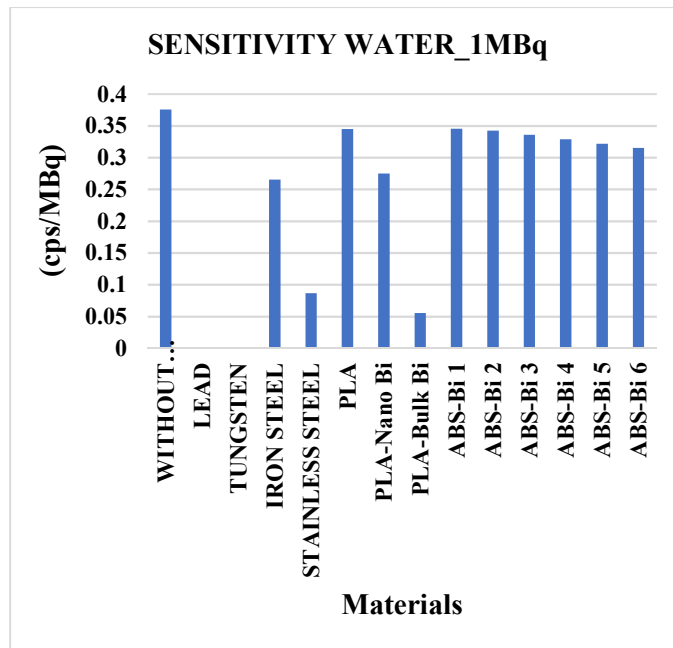


Figure 10: Sensitivity for all Collimator materials at an activity of 1 MBq and energy of 140 KeV of the source 9 Tc-99m.

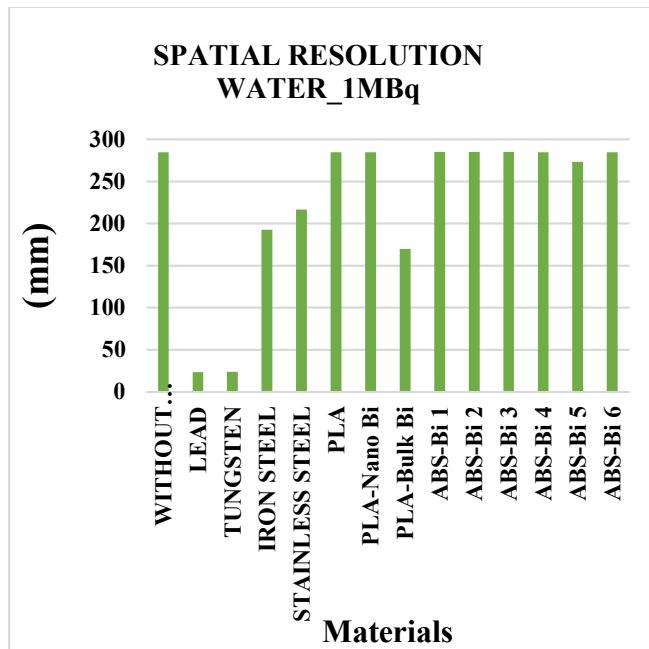


Figure 11: Spatial Resolution for all Collimator materials at an activity of 1 MBq and energy of 140 KeV of the source Tc-99m.

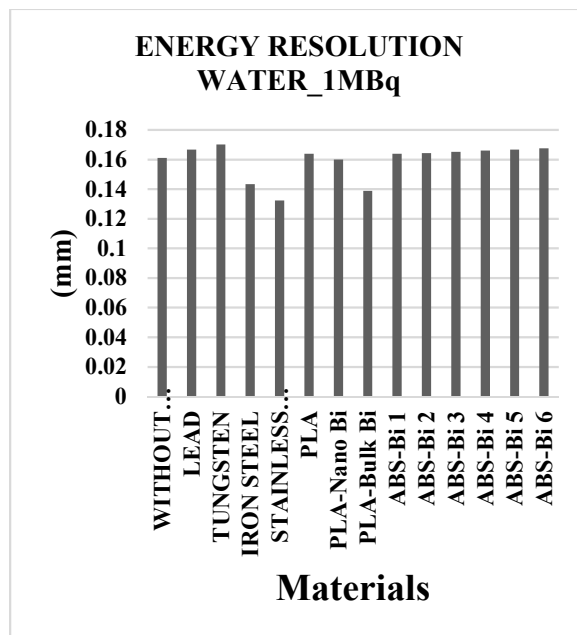


Figure 12: Energy Resolution for all Collimator materials at an activity of 1MBq and energy of 140 KeV of the source Tc-99m.

Discussion

The Monte Carlo simulation results for the Symbian T2 SPECT scanner show significant variations in performance depending on the collimator material used. Materials like "PLA" and "ABS-Bi-2" consistently recorded the highest energy entries and detector counts, demonstrating superior sensitivity. However, spatial resolution varied across materials—"PLA-Nano-Bi" provided good spatial resolution, while "ABS-Bi" showed broader spatial resolutions despite high sensitivity. Tungsten collimators, in contrast, consistently exhibited the lowest energy entries and sensitivity but improved spatial resolution in certain configurations.

In the water phantom study, similar trends emerged, with "iron steel," "PLA," and "ABS-Bi-1" recording the highest energy entries and sensitivity, while tungsten again produced the lowest counts. "PLA" and "ABS-Bi-6" offered the best spatial resolution, and high energy resolution was achieved with "PLA," "ABS-Bi-6," and tungsten. The analysis also highlighted the importance of collimators, as the SPECT head without a collimator had high sensitivity but poor spatial resolution. Ultimately, the study underscores how collimator material choice significantly affects the performance of the SPECT scanner, influencing sensitivity, spatial resolution, and energy resolution.

4. CONCLUSION

The investigation into reinforced Acrylonitrile Butadiene Styrene (ABS) collimators for the Symbian T2 SPECT scanner reveals that materials such as PLA, ABS-Bi-1, ABS-Bi-2, and iron steel provide superior imaging performance, offering high energy entries, detector counts, and sensitivity. These materials also improve spatial and energy resolution, making them optimal choices for SPECT imaging. In contrast, tungsten, while performing well in spatial and energy resolution, consistently underperforms in other key metrics like energy entries and sensitivity.

The study's findings are particularly relevant for low- and middle-income countries (LMICs), where cost-effective materials like PLA and ABS-Bi can enhance diagnostic capabilities without requiring large investments in advanced technologies. By focusing on materials that balance cost with performance, LMICs can improve sensitivity and image quality in SPECT imaging, ultimately leading to better patient outcomes and more effective healthcare delivery. The research also highlights the importance of training healthcare professionals in LMICs to make informed decisions about collimator materials, optimizing imaging performance within available resources.

References

1. Bailey, D.L., Humm, J.L., Todd-Pokropek, A. , Aswegen A. Van (2015). *Nuclear Medicine Physics: A Handbook for Teachers and Students*. IAEA.
2. Bouchard, P. J., & Hsu, J. T. (2016). *Stainless Steel: A Family of Alloys*. *Materials Science Journal*, 12(3), 45-60.
3. Elsafi, M., El-Nahal, M.A., Sayyed, M.I. (2022) Novel 3-D printed radiation shielding materials embedded with bulk and nanoparticles of bismuth. *Sci Rep* 12, 12467.
4. Jha, A. K., & Shankar, R. (2015). "Tungsten: Properties and Applications." *Journal of Materials Science*, 50(2), 1235-1245. doi:10.1007/s10853-014-8297-8.
5. Kijowski, R., & Plewes, D. B. (2019). "Principles and applications of gamma-ray detectors for SPECT." *Journal of Nuclear Medicine Technology*, 45(1), 3-10.

6. Le Rouzic, G., & Zananiri, R. (2021). First performance measurements of a new multi detector CZT-Based SPECT/CT system: *GE StarGuide*. *Journal of Nuclear Medicine*, 62(Supplement 1), 1125.
7. Mina Ouahman, Rachid Errifai, Hicham Asmi, Youssef Bouzekraoui, Sanae Douama, FaridaBentayeb, Faus no Bonu . (2020). Collimator and Energy Window Evaluation in Ga-67 Imaging by Monte Carlo Simulation. *Mol Imaging Radionuclear Ther*;29:118-123.
8. Narayanan, K. B., & Nair, S. V. (2015). "Polylactic Acid: Properties, Structure, and Applications." *Journal of Polymers and the Environment*, 23(3), 335-342. doi:10.1007/s10924-014-0648-4.
9. Patel, S., & Kumar, R. (2016). "Mechanical Properties of Low-Carbon Steels for Structural Components in Radiation Shielding." *Materials Science and Engineering: A*, 661, 47-55.
10. Sarrut D, Bała M, Bardiès M, Bert J, Chauvin M, Chatzipapas K, Dupont M, Etxebeste A, Fanchon LM, Jan S. (2021). Advanced Monte Carlo simulations of emission tomography imaging systems with gate. *Phys MedBiol.*;66(10):10-03
11. Sarrut D, Baudier T, Borys D, Etxebeste A, Fuchs H, Gajewski J, Grevillot L, Jan S, Kagadis GC, Kang HG, (2022). The Open- GATE ecosystem for Monte Carlo simulation in medical physics. *Phys Med Biol.*; 67:184001.
12. Scuiam J W (2012). A CdTe detector for hyperspectral SPECT imaging. *Journal of Instrumentation*. *IOP Journal of Instrumentation*. 7 (8): P08027. doi:10.1088/1748 0221/7/08/P08027. S2CID 250665467.
13. Smith, D. J., & Wang, T. (2017). "Corrosion Behavior of Carbon Steel in Industrial Environments." *Journal of Materials Science*, 52(5), 354-367.
14. Sorenson, J.A., Phelps, M.E., & Thrall, J.H. (2012). *Physics in Nuclear Medicine* (4th ed.). Elsevier. Chapter 16.
15. Wang, J., & Liu, X. (2020). "Improving Image Quality in Gamma Camera Systems: Pulse Height Analysis and Energy Windowing". *Physics in Medicine and Biology*,65(14), 085001.
16. Wernli, R., & de Souza, J. (2018). "Lead and Lead Alloys." *Properties and Selection: Nonferrous Alloys and Special-Purpose Materials*. *ASM Handbook*, Vol. 2.
17. Zhao, W., & Zhang, H. (2019). "Effect of Carbon Content on the Tensile and Fatigue Properties of Carbon Steel Alloys." *Journal of Nuclear Materials*, 513(4), 112-120.